

TURBULENT FLOW IN A CYLINDRICAL CIRCULAR-RECESS CHANNEL

K. N. Volkov, S. V. Denisikhin,
and V. N. Emel'yanov

UDC 532.529

Modeling of a turbulent flow in a cylindrical solid propellant charge channel having a circular recess (compensator) has been performed. Different variants of the compensator position and connection to the channel are discussed. The influence of the geometric and consumption factors on the formation of distributions of the gas-dynamic parameters and characteristics of turbulence in the working region has been investigated.

Introduction. The internal space of the combustion chamber of the solid-propellant rocket engine (SPRE) is a complex system of channels whose walls are formed by the burning surface of the solid propellant charge and the inner surface of the engine case. The SPRE combustion chambers have various geometric designs, which is due to both the solution of arrangement problems and the necessity of providing the mass supply surface required by their operational conditions (control of the combustion surface).

The processes connected with propellant heating and decomposition of its components and their chemical interaction proceed in the thin near-surface layer. The flow of solid propellant combustion products can be described by means of a mathematical model of the flow in an injection channel reflecting the most important aspect of the process — mass supply from the side of the burning charge surface [1–4].

Mass supply channels are present in all designs of the SPRE. The most elementary channel is a cylindrical channel with permeable walls through which a liquid with a constant intensity is injected. For this case theoretical designs are known [1, 2]. The cylindrical channel surface increases during combustion. To compensate for this phenomenon, degressively burning elements, in particular, circular recesses tilted at a certain angle to the channel axis, are introduced into the charge structure. The gas flow thereby proceeds under the conditions of interaction between the main stream in the channel and the crossflow from the slots [5–9].

Channels with a multislot and a star-like shape of the cross-section also find wide application [5–8]. The use of charges with saw cuts (slots) makes it possible to provide a given law of change in the combustion surface in a wide range of pressure change [9].

The problem of gas-dynamic and intraballistic calculation of the SPRE is to find the velocity, pressure, density, and temperature distributions of the flow of combustion products along the length of the internal channel and determine the averaged characteristics of the flow at any instant of time.

Below we consider the problems of numerical modeling of a turbulent flow of solid propellant combustion products in a cylindrical channel with a circular recess (compensator). The influence of the location of the compensating element along the channel length and its angle of inclination on the velocity distributions and the turbulence characteristics in the working region are investigated.

Mathematical Model. The coordinate system is chosen so that the x -axis coincides with the symmetry axis of the channel. The origin of the coordinate system is aligned with the input cross-section of the channel (Fig. 1). As the characteristic length scale, the channel radius R is taken.

The turbulent flow and the heat transfer of the viscous compressible gas are described in an axisymmetric formulation on the basis of the system of equations incorporating the continuity equation, the equation of change in the momentum, and the energy equation, which are closed by the equation of state of the calorically and thermally perfect gas and the equation of the two-parameter k - ε -model of turbulence. The k - ε -model equations take into account correc-

D. F. Ustinov Baltic State Technical University "Voenmekh," 1st Krasnoarmeiskaya Str., St. Petersburg, 190005, Russia; email: dsti@mail.ru. Translated from *Inzhenerno-Fizicheskii Zhurnal*, Vol. 80, No. 6, pp. 116–121, November–December, 2007. Original article submitted December 7, 2005.

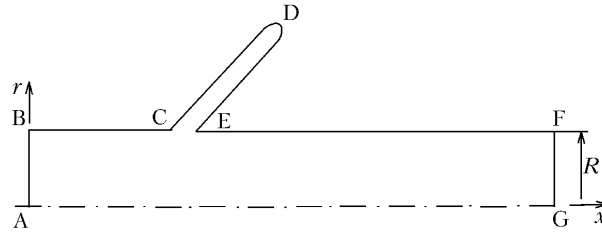


Fig. 1. Geometry of the calculation grid.

tions for the flow rotation (Kato–Launder correction for the term characterizing the generation of turbulence) and corrections for the streamline curvature (a damping function depending on the Richardson number is added to the formula for calculating the turbulent viscosity).

Boundary Conditions. In the inlet cross-section of the channel AB, the velocity distribution is given in the form of the cone-shaped profile [1, 2]

$$u = u_m \cos \left(\frac{\pi r^2}{2 R^2} \right).$$

The maximum velocity $u_m = 150$ m/sec.

On the side surface of the channel BCDEF the boundary condition of normal injection ($u = 0, v = -v_w$) is set. Its velocity is calculated from the condition of equality of the flow rates of consumed fuel and injected gas $\rho_f v_f = \rho_w v_w$, where ρ_f and v_f are, respectively, the charge density and the rate of combustion of the solid fuel; ρ_w and v_w are the density of combustion products and the injection velocity. To find the rate of combustion of the solid fuel, the initial pressure in the channel is given and the rate of combustion and the injection velocity are determined. Then the flow field in the continuous flow channel is calculated and the pressure distribution over the burning surface is found. Then recalculation of the combustion and injection parameters is performed. The process is repeated until convergence is provided.

The turbulence characteristics on the permeable surface of the channel are given constant values ($k = 10^{-3}$ m²/sec², $\epsilon = 10^{-4}$ m²/sec³). The results of the calculations show that the change in the turbulence intensity on the mass-supplying surface in the 0.1–2.5% range does not lead to a significant corruption of the results of numerical modeling.

In the outlet cross-section of the channel FG the boundary conditions of free outflow are given (derivatives on the x -coordinate of all sought functions are equated to zero). On the axis of the channel AG the boundary conditions of flow symmetry are used.

Numerical Method. The Navier–Stokes equations and the equations of the turbulence model are discretized by the control volume approach on a nonstructured grid [10]. For the time discretization of derivatives, the five-step Runge–Kutta method is used. Discretization of convective flows is carried out on the basis of an MUSCL scheme of the third order of accuracy (a minmod flow limiter is used). To discretize diffusion flows, centered difference formulas of the second order of approximation are used.

The system of difference equations is solved by the multigrid method on the basis of the scheme of complete approximation (the V-cycle and four grid levels are used).

Results of the Calculations. The cylindrical channel has a length $L = 1080$ mm and a radius $R = 150$ mm. The width of the recess is 14 mm, and its length is 480 mm.

The calculation grid of the best resolution has 320,000 cells. Nonstructured grids of a lower resolution (three levels) are constructed by the method of collapsing faces [10]. Fragments of the calculation grid corresponding to the compensator and its interface with the channel are shown in Fig. 2.

The working substance represents solid fuel combustion products characterized by the following parameters: $p = 40$ atm, $T = 3000$ K, $G = 306$ kJ/(kg·K), $Pr = 0.442$, $\gamma = 1.17$. The thermophysical properties of the working substance are the reference.

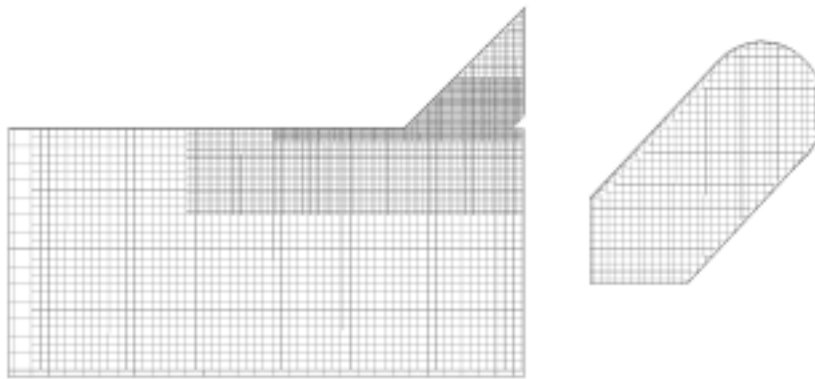


Fig. 2. Fragments of the calculation grid.

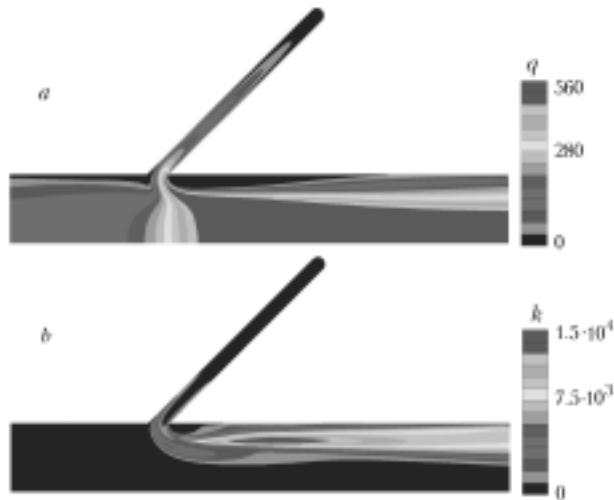


Fig. 3. Lines of the velocity level (a) and kinetic turbulence energy (b) at $\varphi = 45^\circ$. q , m/sec; k , m^2/sec^2 .

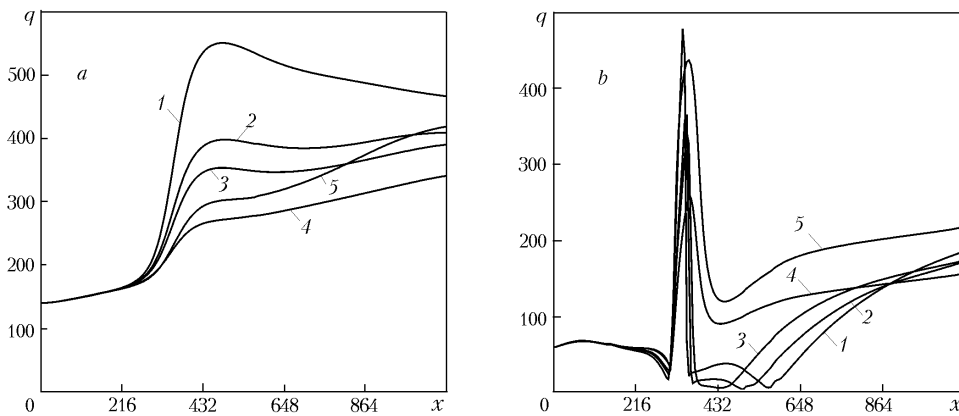


Fig. 4. Velocity distributions in cross-sections of $r/R = 0.5$ (a) and $r/R = 0.9$ (b) at various angles of inclination of the compensator $\varphi = 45^\circ$ (1); 70° (2); 90° (3); 115° (4); 135° (5). q , m/sec; x , mm.

We consider two variants of the compensator position: at the beginning and at the end of the cylindrical channel. The results of the numerical modeling corresponding to the location of the compensator at the beginning of the solid fuel charge channel are given in Figs. 3–8.

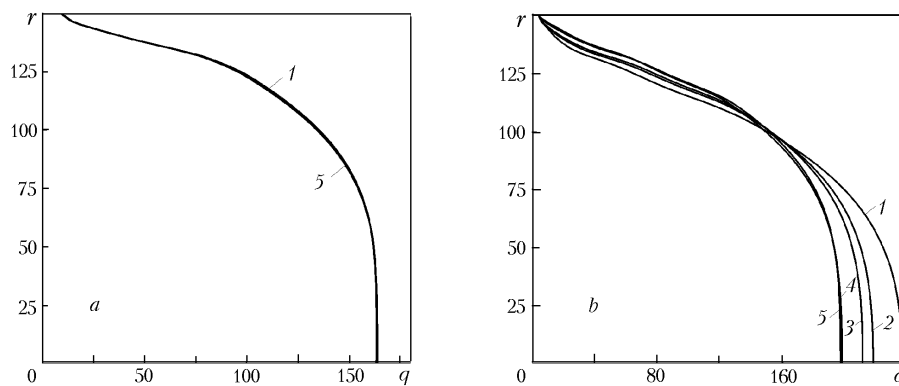


Fig. 5. Velocity distributions in cross-sections of $x/R = 1$ (a) and $x/R = 1.93$ (b): 1–5) notation same as in Fig. 4. r, x , mm.

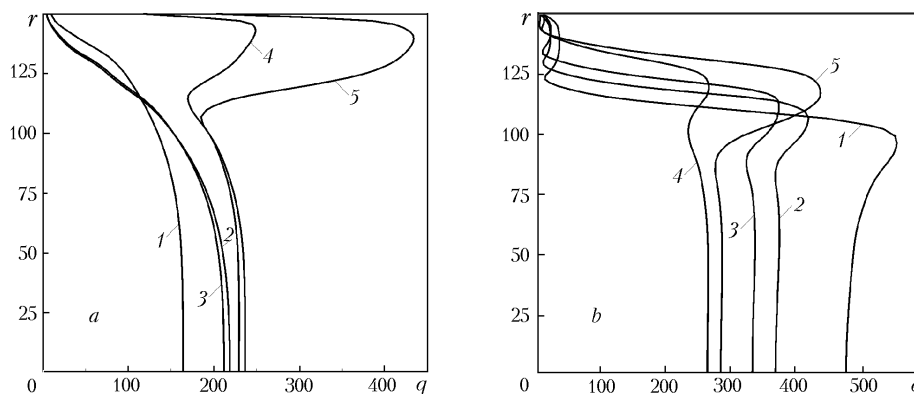


Fig. 6. Velocity distributions in cross-section of $x/R = 2.30$ (a) and $x/R = 2.73$ (b): 1–5) notation same as in Fig. 4. r , mm; q , m/sec.

The presence of a slot leads to a rather strong disturbance of the flow in the channel. However, the latter has a local character — the flow disturbance caused by the interaction between the flow from the slot and the flow in the channel is localized in a relatively small vicinity of the interface between subregions (Figs. 3, 4). With approach to the channel axis (in the range of small values of the radial coordinate) the nonuniformity of the velocity distribution decreases (Fig. 4). Outside the vicinity of this interface the velocity profile in the slot is fairly well described by the cosine dependence [1, 2]. The pressure in the outlet cross-section of the channel is measured within 1.5% of the value that takes place in the absence of a slot.

When the compensator is inclined, near the slot a counterflow region arises, but in this case, too, a considerable restructuring of the flow occurs only near the channel wall. The presence of a compensator has a rather weak effect on the flow structure in the cross-sections situated on the left of the interface between subregions (with decreasing x -coordinate). The degree of influence of the flow from the slot increases with receding from the left boundary of the calculation region (Fig. 5).

If the recess is situated at the beginning of the channel, then in the cross-section just after the recess a considerable nonuniformity of the longitudinal velocity component is observed (Fig. 6). The outflow from the recess forms a high-speed flow, in which the level of the longitudinal velocity component considerably exceeds the velocity on the channel axis in the given cross-section. Downstream, the local maximum of the longitudinal velocity component moves to the axis, since the flow from the recess is pressed back by the gas flowing from the permeable surface of the channel (Fig. 7). At a considerable distance from the recess in the longitudinal direction the velocity profile smoothes, approaching a cosine distribution. But when the recess is situated in the part of the charge that faces the nozzle cap, the channel flow has a high level of longitudinal velocity and a local velocity maximum is not formed.

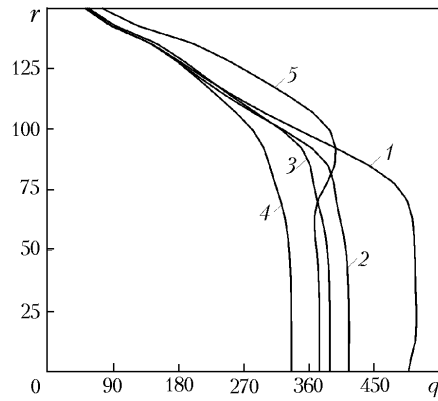


Fig. 7. Velocity distributions in cross-sections of $x/R = 5.9$: 1–5) notation same as in Fig. 4. r , mm; q , m/sec.

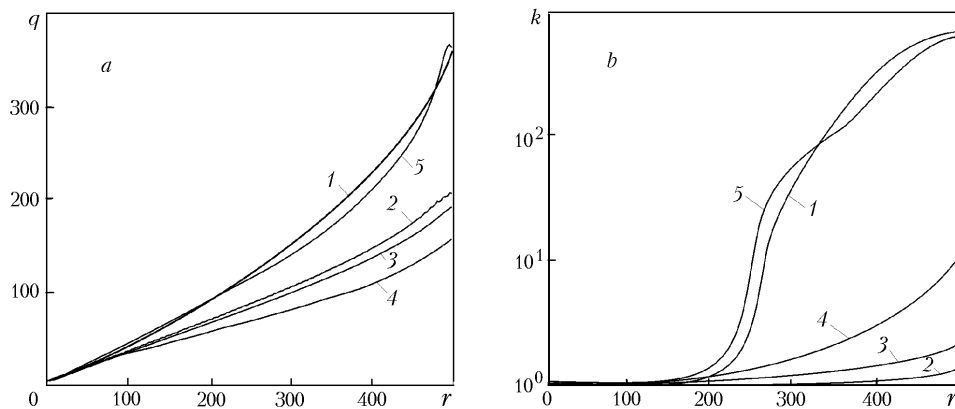


Fig. 8. Distributions of the velocity (a) and the kinetic turbulence energy (b) in the compensator: 1–5) notation same as in Fig. 4. q , m/sec; k , m^2/sec^2 ; r , mm.

In both cases, the additional flow from the slot into the channel leads to the formation of a velocity profile filled to a greater extent (compared to the cosine profile).

If the slot is situated at the beginning of the channel where the mainstream flow velocities are not yet high, more disturbances caused by the injection from the side surface of the compensator penetrate into the mainstream flow. In accordance with the indicated intensity of flow field distortion, intensification of the processes of interphase interaction (in modeling two-phase flows) may be expected.

The calculations show that the presence of a local maximum of the longitudinal velocity component induced by the mass-supplying element-recess and its value are determined by the intensity of the additional gas input and the flow section of the mass-supplying element at its interface with the channel. In particular, the local velocity maximum becomes appreciable when the average velocity from the recess-type element exceeds the average velocity on the channel cross-section at the junction. For instance, if we denote by d_c and S_c the diameter of the channel and its surface of gas supply to the junction and by b and S_e the width of the junction zone and the surface of the element, then the condition for the appearance of a local maximum is given by the relation

$$\frac{S_e}{b} \geq \frac{S_c}{d_c}.$$

In some cases, the gas input surface is formed from a sequence of axisymmetric grooves. Such channels are used in systems where developed combustion surfaces are required. Considerable deformations of the longitudinal velocity profile are observed in the initial cross-sections of the channel. As the longitudinal coordinate increases, the ve-

locity profile smoothes and at large distances from the inlet boundary it becomes close to the cosine distribution and the action of the mass-supplying elements becomes equivalent to the increase in the injection intensity.

As the gas arrives through the side walls, the flow velocity increases. In the area adjoining the initial cross-section of the channel, the gas compressibility can be neglected. The distribution of the axial velocity component over the cross-section of the channel is fairly well described by the cosine dependence, and the dependence of the pressure on the distance x is practically parabolic [3, 4].

Downstream, the axial flow intensity increases. As soon as the momentum becomes approximately equal to the axial component of the momentum transferred by the gas flowing away from the walls, the gas particles from the mainstream flow will begin to penetrate to the wall and slow down near it. In so doing, a boundary layer arises, which thickens and fills the cross-section of the channel. As the x -coordinate increases further, the influence of viscous effects covers the whole of the cross-section of the channel.

With increasing injection velocity there occurs turbulization of the flow (due to the increase in the velocity gradient in the central part of the channel), except for the near-wall and near-axis regions, and the pulsation energy maximum shifts from the wall into the flow. There appears a tendency for a decrease in the pulsation intensity in the flow core, and near the channel surface a wall layer (pressing-back zone), in which the flow is similar in properties to a laminar flow, is formed.

Conclusions. On the basis of Reynolds-averaged Navier–Stokes equations the influence of geometric and consumption factors on the formation of the flow pattern in a cylindrical channel with a circular recess has been investigated.

It has been shown that the flow disturbance in the cylindrical channel caused by the presence of a circular recess has a local character and is localized in a small vicinity of the interface between the slot and the solid fuel charge channel. The intensity of the flow disturbances in the channel introduced by the recess and the position and presence of the local maximum of the longitudinal velocity component depend on the position of the recess (at the beginning of the channel or at its end) and the angle of inclination of the compensator.

The results of the calculations can be used for subsequent simulation of the motion of condensed-phase particles and their interaction and separation.

NOTATION

b , width of the interface between the circular recess and the channel, m; d , diameter, m; G , gas constant, J/(kg·K); k , kinetic energy of turbulence, m^2/sec^2 ; L , length, m; p , pressure, Pa; Pr, Prandtl number; q , velocity value, m/sec; r , radial coordinate, m; R , radius, m; S , area, m^2 ; T , temperature, K; u , axial velocity component, m/sec; v , radial velocity component, m/sec; x , longitudinal coordinate, m; γ , ratio between specific heat capacities; ε , dissipation rate of kinetic turbulence energy, m^2/sec^3 ; ρ , density, kg/m^3 ; φ , angle of inclination of the compensator. Subscripts: c, channel; e, mass-supplying element; f, fuel; m, maximum; w, wall.

REFERENCES

1. V. M. Eroshenko and L. I. Zaichik, *Hydrodynamics and Heat and Mass Transfer on Permeable Surfaces* [in Russian], Nauka, Moscow (1984).
2. B. A. Raizberg, B. T. Erokhin, and K. P. Samsonov, *Fundamentals of the Theory of the Working Processes in Solid-Propellant Rocket Systems* [in Russian], Mashinostroenie, Moscow (1972).
3. A. M. Lipanov (Ed.), *A Numerical Experiment in the Theory of Solid-Propellant Rocket Engines* [in Russian], Nauka, Ekaterinburg (1994).
4. A. A. Shishkov, S. D. Panin, and B. V. Romyantsev, *Working Processes in Solid-Propellant Rocket Engines* [in Russian], Mashinostroenie, Moscow (1989).
5. V. N. Emel'yanov, Physical and computational modeling of three-dimensional flows in propulsion systems, in: *Intrachamber Processes, Combustion, and Gas Dynamics of Disperse Systems* [in Russian], BGTU, St. Petersburg (1996), pp. 124–137.

6. V. N. Emel'yanov, Internal complex-structure flows, in: *Intrachamber Processes, Combustion, and Gas Dynamics of Disperse Systems* [in Russian], BGTU, St. Petersburg (1998), pp. 80–91.
7. K. N. Volkov and V. N. Emel'yanov, Three-dimensional turbulent flows in injection, channels in: V. N. Uskov (Ed.), *Current Problems of Nonequilibrium Gas- and Thermodynamics* [in Russian], BGTU, St. Petersburg (2002), pp. 43–63.
8. K. N. Volkov and V. N. Emel'yanov, Mathematical models of three-dimensional turbulent flows in injection channels, *Mat. Modelir.*, **16**, No. 10, 41–63 (2004).
9. A. D. Rychkov, *Mathematical Modeling of Gas-Dynamic Processes in Channels and Nozzles* [in Russian], Nauka, Novosibirsk (1988).
10. K. N. Volkov, Application of the control-volume method for solving problems of the mechanics of liquids and gases on nonstructured grids, *Vychisl. Metody Programmir.*, **6**, No. 1, 43–60 (2005).